Available online at www.sciencedirect.com
ScienceDirect
European Journal of Pharmaceutics and Biopharmaceutics 69 (2008) 445–453
European Journal of Pharmaceutics and Biopharmaceutics
www.elsevier.com/locate/ejpb

Research paper

Dual agents loaded PLGA nanoparticles: Systematic study of particle size and drug entrapment efficiency

Xiangrong Song [a,b], Yu Zhao [c], Shixiang Hou [a,*], Fangyuan Xu [a], Rongli Zhao [a], Junyao He [a], Zheng Cai [a], Yuanbo Li [a], Qiuhong Chen [a]

[a] West China School of Pharmacy, Sichuan University, Sichuan, PR China
[b] State Key Laboratory of Biotherapy, Sichuan University, Sichuan, PR China
[c] Department of Central Nervous System, Shanghai, PR China

Received 24 September 2007; accepted in revised form 15 January 2008
Available online 19 January 2008

Abstract

PLGA nanoparticles simultaneously loaded with vincristine sulfate (VCR) and quercetin (QC) were prepared via O/W emulsion solvent evaporation. Six independent processing parameters and PLGA characteristics were assessed systematically to enhance the incorporation of the dual agents with different properties (VCR and QC, hydrophilic and hydrophobic molecule, respectively) into PLGA nanoparticles and control particle size. Approaches investigated for the enhancement of drug entrapment efficiencies and the controlling of particle size included the influence of the molecular weight (MW) of PLGA and the lactide-to-glycolide (L:G) ratio of PLGA, PLGA concentration, PVA concentration, initial QC content, acetone-to-dichloromethane (A/D) volume ratio, aqueous phase pH and aqueous to organic phase (W/O) volume ratio. The nanoparticles produced by optimal formulation were submicron size (139.5 ± 4.3nm, $n = 3$) with low polydispersity index (0.095 ± 0.031, $n = 3$). Nanoparticles observed by transmission electron microscopy (TEM) showed extremely spherical shape. The entrapment efficiencies determined by high performance liquid chromatography (HPLC) by ultracentrifuge method were $92.84 \pm 3.37\%$ for VCR and $32.66 \pm 2.92\%$ for QC ($n = 3$). The drug loadings were $0.0037 \pm 0.0001\%$ for VCR and $1.36 \pm 0.12\%$ for QC ($n = 3$).

Keywords: Vincristine sulfate; Quercetin; PLGA; Nanoparticles; O/W

1. Introduction

Multidrug resistance (MDR), whereby cancer cells become resistant to the cytotoxic effects of various structurally and mechanistically unrelated chemotherapeutic agents [1], is a major problem in the clinical treatment of cancer. Vincristine sulfate (VCR) is an effective chemotherapeutic agent, which has been used extensively for treatment of various cancers including AIDS-KS [2]. Unfortunately, many tumor cells are not sensitive to VCR because of efflux from the tumor cells mediated by P-glycoprotein (Pgp), multidrug resistance-associated protein 1 (MRP1), MRP2 and MRP3 [3,4]. Quercetin (QC), a kind of natural flavone, has been reported to be able to reverse resistance caused by Pgp [5], MRP1 [6], MRP4 [7], MRP5 [7] and BCRP/ABCG2 [8] at concentrations of approximately 9–44 μM/L. In comparison to the early generation of chemosensitizers (e.g. cyclosporin-A, verapamil), QC has a higher potency for several kinds of proteins associated with MDR [9]. However, the in vivo reversal efficacy of QC might not be satisfactory when it was administered systemically via free drug due to its high binding ratio of drug–plasma protein (99.4%) [10]. Meanwhile, VCR also has severe neurotoxicity when administered systemically [11]. One way to decrease the toxicity

* Corresponding author. West China School of Pharmacy, Sichuan University, No. 17, Section 3, Renmin Nan Road, Chengdu, Sichuan 610041, PR China. Tel./fax: +86 28 85502809.
E-mail address: housix@263.net (S. Hou).

0939-6411/$ - see front matter © 2008 Elsevier B.V. All rights reserved.
doi:10.1016/j.ejpb.2008.01.013

of VCR and increase the in vivo reversal efficacy of QC is encapsulating them in nanoparticles that are capable of targeting tumor tissues or cells and changing their in vivo distributive characteristics. Julia et al. [12] found that the administering sequence of antitumor agent and chemosensitizer would affect the efficacy of resistance reversion. The previous research performed by Elaine et al. [6] also proved that simultaneous administration of VCR and QC could result in better treatment efficacy. Thus, it may be preferable to prepare nanoparticles incorporated with both VCR and QC so that the two substances could be delivered simultaneously.

A recently published study demonstrated that MDR mediated by Pgp could be reversed by encapsulating anticancer drug in transferrin-conjugated poly(D,L-lactide-co-glycolide) (PLGA) nanoparticles [13]. Thus, PLGA nanoparticles were chosen as carriers in this study. Encapsulating VCR and QC in PLGA nanoparticles might overcome MDR through the chemosensitizer QC and the carrier PLGA nanoparticles.

In recent two decades, PLGA has been extensively used in drug delivery systems for a variety of drugs due to its excellent biocompatibility and biodegradability [14,15]. PLGA nanoparticles have also attracted considerable attention and interest. Current literature is replete with studies investigating single-agent incorporation into PLGA nanoparticles [16–19], while PLGA nanoparticles loaded with dual agents were reported scarcely [20]. In this study, VCR and QC are hydrophilic and hydrophobic molecules, respectively. Owing to the obviously different properties of the two drugs, to prepare the two drugs loaded PLGA nanoparticles with high drug entrapment efficiency using the adapted preparation method represents a real challenge. The commonly reported preparation methods of PLGA nanoparticles include emulsion solvent evaporation [20,21], nanoprecipitation [17], solvent displacement [22] and salting-out [23]. Taking into account of the properties of VCR and QC and the simplification of preparation process, the O/W single emulsification method was selected for this study.

According to literatures [24,25], nanoparticles larger than 200 nm can be mechanically filtered in the spleen while those smaller than 100 nm left the blood vessels through fenestrations in the endothelial lining. Thus, to deliver drugs to tumor, nanoparticles with relatively small size in the range of 100–200 nm were desirable. The main aim of this study was to optimize the incorporation of VCR and QC into PLGA nanoparticles by O/W single emulsification method to produce enhanced drug entrapment efficiency. The formulation parameters were systematically investigated. Therefore, nanoparticles with some expectable properties such as high-drug entrapment efficiency and suitable size can be produced through the optimized formulation. Following that, the physicochemical characteristics were also evaluated, which can provide some useful and essential information for in vitro cell experiments and in vivo studies.

2. Materials

Different types of PLGA (shown in Fig. 1a) were purchased from Department of Medical Polymers, Shandong Institute, China. PVA205 (88% of hydrolyzation degree, 500 of polymerization degree) was purchased from Kuraray Co., Ltd., China. VCR (purity 98%) was purchased from Huanye Pharmaceutical Co., Ltd. (Guangzhou, China). Quercetin dihydrate (QC, purity 98%) was obtained from Okay Plant Chemical Co., Ltd. (Chengdu, China). All other chemicals and solvents were of reagent grade.

2.1. Nanoparticle preparation

PLGA nanoparticles loaded with VCR and QC were prepared using a modified version of an o/w single-emulsion solvent evaporation process [26]. The organic phase consisted of PLGA polymer and drugs dissolved in an acetone–dichloromethane mixture. The aqueous phase contained PVA solution. The organic phase was emulsified with the aqueous phase by sonication using a microtip probe sonicator (JY88-II ultrasonic processor, China) at an output of 50 W for 30 s in ice bath. The organic mixture was then rapidly removed by evaporation under reduced pressure at 37 °C leaving behind colloidal suspension of PLGA nanoparticles (VQ-PLGA-NPs) in water.

In this study, the effect of various process parameters and polymer characteristics on nanoparticles mean diameter and drug entrapment efficiencies were assessed, including the molecular weight (MW) of PLGA and the lactide-to-glycolide (L:G) ratio of PLGA, PLGA concentration in the organic phase, PVA concentration in the aqueous phase, initial QC content, acetone-to-dichloromethane (A/D) volume ratio, aqueous phase pH and aqueous-to-organic phase (W/O) volume ratio. Unless otherwise mentioned, all the experiments were conducted by varying one of the parameters while keeping all the other process parameters at a set of standard conditions: 20 mg/ml of PLGA 75:25, MW 15 kDa, 10 μM of VCR and 10 mM of QC in 1.5 ml of acetone–dichloromethane mixture (1:2, v/v) as the organic phase, and 4.5 ml of 2% PVA205 solution as the aqueous phase. The aqueous-to-organic phase volume ratio was 3:1 and polymer-to-drug ratio was 5:1 (PLGA/QC, w/w). All batches of nanoparticles were produced at least in triplicate.

2.2. Determination of entrapment efficiencies and drug loadings of VCR and QC

To separate the free VCR and QC in the supernatant from the nanoparticles, the nanoparticle suspension was ultracentrifuged for 1 h at 4 °C and 223,000*g* (Optima MAX-E Ultracentrifuge, Beckman Coulter Inc., USA). The supernatant was removed and nanoparticles sediments were washed twice with 2% PVA205 solution in order to remove the adsorbed drugs. The washing solution was

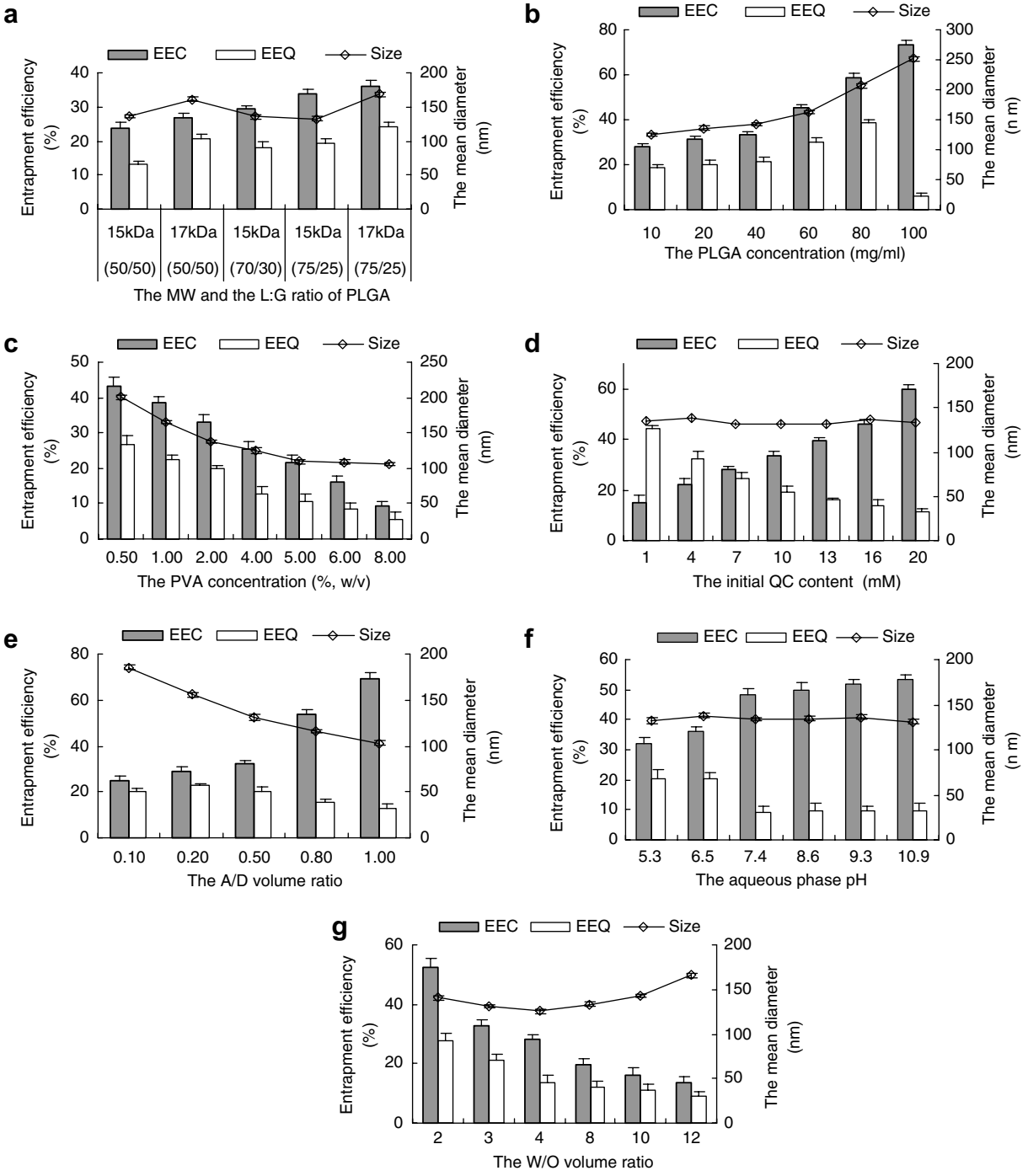

Fig. 1. Effect of various processing parameters and polymer characteristics on the mean diameter and drug entrapment efficiencies of nanoparticles, including the molecular weight (MW) of PLGA and the lactide-to-glycolide (L:G) ratio of PLGA (a), PLGA concentration in the organic phase (b), PVA concentration in the aqueous phase (c), initial QC content (d), acetone to dichloromethane (A/D) volume ratio (e), aqueous phase pH (f) and aqueous to organic phase (W/O) volume ratio (g) ($n = 3$). The abbreviations of the entrapment efficiency of VCR and QC are EEC and EEQ, respectively.

eliminated by a further ultracentrifugation as described above. And then, 5 ml of dimethylsulfoxide was added into the sediments and the mixture was vortexed for 5 min. After centrifugation at 76*g* for 10 min, 20 μl of supernatant was injected into an Agillent 1100 liquid chromatograph to determine the actual amounts of VCR and QC incorporated within the nanoparticles. Separation was achieved using a Diamonsil C18 column (250 mm × 4.6 mm, 5 μm, Dikma Technologies, Beijing, China) at a flow rate of 1.0 ml/min and a detection of 297 nm. All the analysis was performed at 37 °C. To determine the total amount of VCR and QC in the nanoparticle suspension, 500 μl of nanoparticle suspension was mixed with 4.5 ml of dimethylsulfoxide for 5 min by sonication. After centrifugation at

76*g* for 10 min, supernatant was determined by HPLC analysis.

The entrapment efficiencies (EE) of VCR and QC could be calculated with the percent ratio of the actual amounts of VCR and QC incorporated into nanoparticles to the total amounts of VCR and QC in nanoparticle suspension. The drug loadings (DL) of VCR and QC could be also calculated as the actual amount of VCR and QC incorporated into nanoparticles versus the total amount of the freeze-dried VQ-PLGA-NPs. Experiments were performed in triplicate.

2.3. Particle size and zeta potential

Particle size and polydispersity index were determined by photon correlation spectroscopy (PCS) using Zetasizer Nano ZS90 (Malvern Instruments Ltd., Malvern, UK). Size measurements were performed in triplicate following a 1/100 (v/v) dilution of the nanoparticle suspension in redistilled water at 25 °C. The polydispersity index ranged from 0 to 1. Zeta potential was measured using the same instrument at 25 °C following the same dilution in an 1 mM/L NaCl solution. Each measurement was done in triplicate.

2.4. Transmission electron microscopy (TEM)

The morphology of the VQ-PLGA-NPs was examined by TEM (H-600, Hitachi, Japan). Before analysis, the samples were diluted 1:5 and stained with 2% (w/v) phosphotungstic acid for 30 s and placed on copper grids with films for observation.

2.5. Differential scanning calorimetry (DSC)

The physical state of VCR and QC loaded in VQ-PLGA-NPs was investigated by DSC (DSC 200PC, Netzsch, Germany) under nitrogen atmosphere at flow rate of 20 ml/min. Ten milligrams of freeze-dried nanoparticles was heated from 10 to 300 °C at speed of 10 °C/min. VCR, QC, blank nanoparticles and the physical mixture of the three substances (the proportion was consistent with that in optimized VQ-PLGA-NPs) were treated as controls.

2.6. In vitro release

In vitro release studies of VCR and QC from VQ-PLGA-NPs were carried out at 37 ± 1 °C by the dialysis bag technique. Briefly, 1 ml of VQ-PLGA-NPs suspension without free drugs (removed by ultracentrifugation) was put in dialysis sac, and the dialysis sac was placed in 10 ml, pH 7.4 phosphate buffer solution to maintain the sink condition and shaken in a constant temperature shaker (Taicang biochemical instrument industry, Jiangsu, China) at 70 rpm. At regular time intervals, 0.5 ml of the release medium was removed and replaced with 0.5 ml of the fresh release medium. The samples were subjected to HPLC assay. Experiments were performed in triplicate. A control experiment to determine the release behavior of the free drug was also performed in the same way with the same proportion of VCR and QC as it is in VQ-PLGA-NPs.

2.7. Data analysis

Multivariate data analysis was performed by multiple linear regression on Statistical Product and Service Solutions (SPSS V13.0, SPSS Inc., Chicago, USA).

3. Results and discussion

3.1. Effect of preparation variables on formulation characteristics

In this study, the effect of eight preparation variables on the mean diameter and entrapment efficiencies of VQ-PLGA-NPs was investigated. The results are shown in Fig. 1(a–g) and Table 1. The mean diameter of VQ-PLGA-NPs increased with the increase of MW of PLGA and PLGA concentration, but decreased with the increase of PVA concentration and A/D volume ratio. From Table 1, we could conclude that L:G ratio of PLGA, initial QC content and aqueous phase pH had no significant effect on the mean diameter. The results of statistical analysis showed that MW of PLGA, PLGA concentration, PVA concentration and A/D volume ratio were the dominant factors ($p < 0.05$, respectively) in controlling the particle size.

As described in Fig. 1(a–g) and Table 1, the entrapment efficiencies of VCR had a positive relationship with MW of PLGA, L:G ratio of PLGA, PLGA concentration, initial QC content, A/D volume ratio and aqueous phase pH; and a negative relationship with PVA concentration and W/O volume ratio. While the entrapment efficiencies of QC had a positive relationship with MW of PLGA, L:G ratio of PLGA and PLGA concentration; and a negative relationship with PVA concentration, initial QC content, A/D volume ratio, aqueous phase pH and W/O volume

Table 1
The relationship of various formulation parameters with the mean diameter and drug entrapment efficiencies of nanoparticles

Formulation parameters	Mean diameter	Entrapment efficiencies	
		VCR	QC
MW of PLGA	+*	+*	+
L:G ratio of PLGA	○	+*	+
PLGA concentration	+*	+*	+*
PVA concentration	−*	−*	−*
Initial QC content	○	+*	−*
A/D volume ratio	−*	+*	−
Aqueous phase pH	○	+*	−*
W/O volume ratio	− +	−*	−*

+, means positive correlation, −, means negative correlation, ○, means no correlation, *, means significance ($p < 0.05$).

ratio. The results of multiple linear regression analysis illustrated that PVA concentration, initial QC content, aqueous phase pH and W/O volume ratio were the main variables ($p < 0.05$, respectively) in generating particles entrapped with high amount of VCR and QC.

3.1.1. PLGA characteristics

The influence of MW of PLGA and L:G ratio of PLGA on the mean diameter and entrapment efficiencies of VQ-PLGA-NPs was investigated. The results are presented in Fig. 1a. It can be seen that the mean diameter was not affected by L:G ratio of PLGA but influenced obviously by MW of PLGA. The mean diameter increased dramatically with the increase of MW of PLGA ($p < 0.05$). Increasing MW of PLGA resulted in the increase of the viscosity of internal phase, thereby decreasing the net shear stress and increasing the particle size. In our previous research [20], we found that MW of PLGA influenced the particle size slightly, which did not agree well with the result in this study. This phenomenon can be expected from different drug ingredients. In this study, we replaced the hydrophilic molecule VRP with the hydrophobic molecule QC. At the presence of QC, the particle size was probably more sensitive to the change of MW of PLGA.

Fig. 1a shows that the entrapment efficiencies of two drugs increased with the increase of MW and L:G ratio of PLGA. When the MW of PLGA increased, the entrapment efficiencies of two drugs increased slightly, which probably resulted from the increase of nanoparticle size [20,21]. Increase in particle size, with the increase of MW of PLGA, can increase the length of diffusional pathways of drugs from the organic phase to the aqueous phase, thereby reducing the drug loss through diffusion and increasing the drugs' entrapment efficiencies. As the amount of lactide of PLGA increased, the entrapment efficiency of VCR increased significantly ($p < 0.05$) while the entrapment efficiency of QC increased slightly. With the increase of L:G ratio of PLGA, the interaction or affinity of both drugs with PLGA probably increased [16,27]. The interaction or affinity of VCR with PLGA increased more dramatically than that of QC with PLGA, thus the entrapment efficiency of VCR changed more obviously.

3.1.2. PLGA concentration in the organic phase

Fig. 1b shows that the mean diameter of nanoparticles increased dramatically with the increase of PLGA concentration ($p < 0.05$). Increasing PLGA concentration led to increase in the viscosity of the organic phase, hence reducing the net shear stress and promoting the formation of droplets with larger size. In addition, the increasing viscosity could hinder rapid dispersion of PLGA solution into the aqueous phase, resulting in larger droplets which formed larger nanoparticles after elimination of the organic solvent. Moreover, with the increase of the amount of PLGA, PVA was probably insufficient to cover the surface of droplets completely, which caused the coalescence of droplets during the evaporation of organic solvent and aggregation of nanoparticles after the removal of organic solvent.

Fig. 1b shows the effect of PLGA concentration on the entrapment efficiencies of two drugs. The entrapment efficiency of VCR increased significantly ($p < 0.05$) with the increase of PLGA concentration, while the entrapment efficiency of QC first increased and then decreased. This phenomenon probably resulted from the increase of viscosity. Increasing viscosity could increase the drugs resistance diffusional into the aqueous phase and thus enhance the drugs incorporation into nanoparticles. Additionally, as discussed above, larger nanoparticles had higher drug entrapment efficiencies. When PLGA concentration reached 100 mg/ml, the entrapment efficiency of QC was lowest ($6.04 \pm 1.21\%$). This can be attributed to the adsorption of drug molecules on the nanoparticle surface. As the particle size was too large, more hydrophobic molecule QC was probably easy to adsorb onto the large surface of nanoparticles, thereby leading to less amount of QC entrapped into nanoparticles.

3.1.3. PVA concentration

Fig. 1c shows that the mean diameter first decreased dramatically and then reached a plateau with increasing PVA concentration ($p < 0.05$). At high concentration, more PVA can be oriented at organic solvent/water interface to reduce efficiently the interfacial tension [28], which resulted in significant increase in the net shear stress at a constant energy density [29,30] during emulsification and promoted the formation of smaller emulsion droplets. Thus, the mean diameter of nanoparticles decreased with the increase of PVA concentration. However, with the increase in PVA concentration, the viscosity of the external aqueous phase increased, which resulted in size increase due to decrease in the net shear stress [21]. The change in the mean diameter with PVA concentration in this study was predominantly a result of reduction of the interfacial tension which dominated over the increasing viscosity. At the concentration of 5%, the amount of PVA was sufficient to cover the emulsion droplets completely. Therefore, during the removal of organic solvent, PVA can avoid the coalescence of droplets and then cause the formation of nanoparticles with smaller size. After the removal of organic solvent, more PVA molecules can be physically incorporated onto the NP surface [28,31], and then a large number of hydroxyl groups extending into the continuous phase could be hydrated, hence forming a hydrated layer at the surface to hinder nanoparticle aggregation.

Similarly, the entrapment efficiencies of two drugs decreased significantly with the increase of PVA concentration as described in Fig. 1c ($p < 0.05$). That was probably caused by the decrease in particle size. Moreover, with the increase of PVA concentration, more molecules of two drugs may partition out rapidly into the aqueous phase during emulsification procedure and less drug molecules remained in emulsion droplets to interact with PLGA molecules, hence decreasing the entrapment efficiencies.

Additionally, we found that PVA at high concentration can dramatically increase the solubility of QC in aqueous solution in our previous experiment. Therefore, less QC molecules remained in the internal phase to interact with PLGA molecules when the external and internal phase were mixed.

3.1.4. Initial QC content

Fig. 1d shows that the initial QC content had no substantial effect on the nanoparticle mean size, which was similar to hydrophobic drug–PLGA system [21,32] and dual agent–PLGA system [20]. In contrast, the increase of the initial QC content resulted in a significant reduction in entrapment efficiency of QC ($p < 0.05$) but an obvious increase in entrapment efficiency of VCR ($p < 0.05$). The decreasing entrapment efficiency of QC was possibly caused by the nonlinear increase of QC amount entrapped into nanoparticles with the increase of the initial QC content, as shown in Fig. 2. With increase in initial QC content, the QC concentration in the organic phase increased and then more drug molecules could interact with PLGA molecules, resulting in the increase of the entrapment amounts of VCR and QC. Nevertheless, the increase of the entrapment amounts of drugs was not in proportion to the increase of initial drug content, thus the entrapment efficiencies decreased. As the initial QC content increased, the amount of VCR partitioned into the aqueous phase probably reduced during emulsification procedure. Thus more VCR molecules could remain in emulsion droplets to interact with PLGA molecules and the entrapment of VCR could be further enhanced. In this study, QC improved the entrapment of VCR probably by acting as NaCl in the preparation of VV-PLGA-NPs [20].

3.1.5. Acetone-to-dichloromethane volume ratio

Fig. 1e shows the obvious reduction of mean diameter with A/D volume ratio increasing ($p < 0.05$). Acetone is a freely water-miscible organic solvent. When A/D volume ratio increased, the rapid dispersion of considerable amount of acetone into the external aqueous phase contributed to a significant decrease of the interfacial tension, thereby decreasing the particle size.

The entrapment efficiency of VCR increased dramatically with the increase of A/D volume ratio ($p < 0.05$) while that of QC decreased progressively, as presented in Fig. 1e. This occurred possibly because the change of A/D volume ratio affected the partition of two drugs in the organic phase. The hydrophobic molecule QC was easy to dissolve in acetone. When A/D volume ratio reached 0.8, more QC molecules were carried into the aqueous phase or at organic solvent/water interface by considerable amount of acetone; and thus less QC molecules remained in the internal phase to interact with PLGA molecules and lower entrapment efficiency was obtained. As discussed in our previous paper, increase in A/D volume ratio would increase the partition of VCR in the organic phase. In addition, increasing partition of QC in the aqueous phase might act as NaCl and increase the partition of VCR in the organic phase as discussed above. Hence, more VCR molecules interacted with PLGA molecules in the internal phase and enhanced entrapment was carried out.

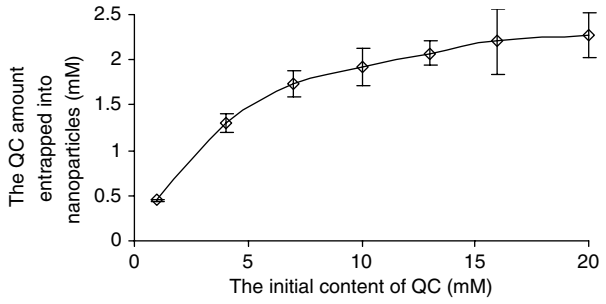

Fig. 2. Effect of initial QC content on the amount of QC entrapped into nanoparticles.

3.1.6. Aqueous phase pH

According to literatures [20,33], adjusting aqueous phase pH could enhance the incorporation of water-soluble drug. In order to provide information about the effect of the aqueous phase pH on mean diameter and drug entrapment efficiencies, studies were subsequently performed using external phase with different pH values adjusted by NaOH. The results are presented in Fig. 1f. The mean diameter of nanoparticles was independent of the aqueous phase pH, while the entrapment efficiencies of two drugs changed significantly with the increasing aqueous phase pH. As the aqueous phase pH increased, the entrapment efficiency of VCR increased dramatically ($p < 0.05$) while that of QC decreased significantly ($p < 0.05$). When the aqueous pH increased, the ionization degree of VCR probably reduced [33] and then more drug molecules without ionization could be retained in the hydrophobic nanoparticle matrix, thereby enhancing the entrapment of VCR. While the aqueous pH approached 7.4, the entrapment efficiency of QC reduced obviously. We considered this that at higher pH especially above pK_a (7) of QC [34], more QC molecules ionized. Owing to ionization, the partition of QC in the internal phase decreased and then less QC molecules interacted with PLGA molecules. In addition, the interaction/affinity of ionized QC with PLGA was low, thus leading to lower entrapment efficiency of QC.

3.1.7. Aqueous-to-organic phase volume ratio

Fig. 1g shows that the mean diameter first decreased and then increased with increase in W/O volume ratio. When W/O volume ratio increased, the amount of PVA increased, resulting in reduction of interfacial tension and thereby decreasing the nanoparticle size, as discussed above. On the other hand, the increased volume of system would reduce the net shear stress due to a constant external energy input, leading to increase in particle size [35]. The particle size was determined by the two competitive effect of W/O volume ratio, namely, the mean diameter first decreased because the former dominated over the latter

and then increased because the latter dominated over the former.

As shown in Fig. 1g, the mean entrapment efficiencies of these two drugs decreased dramatically with the increase of W/O volume ratio ($p < 0.05$). This occurred because the amount of drugs partitioned into the organic phase reduced during emulsification, meanwhile, the drug loss increased during solvent evaporation when the W/O volume ratio increased. Moreover, when W/O volume ratio increased, the amount of QC dissolved in the aqueous phase, resulting in less QC retention in the internal phase to interact with PLGA molecules and then lower entrapment efficiency of QC.

3.2. Optimization of VQ-PLGA-NPs

Leslie et al. [6] reported that 10 μM/L of QC can reverse completely the resistance of MRP1-overexpressing HeLa cells to 10 nM/L of VCR. The molar ratio of VCR-to-QC in the above mentioned experiment was 1/1000, but QC had a lower entrapment efficiency than VCR as described above, so the molar ratio of VCR-to-QC in the initial drug content must be adjusted. Taking high entrapment efficiencies of these two drugs and small particle size into account, we prepared VQ-PLGA-NPs as follows: 80 mg of PLGA (75:25, 15,000), 3.5 μM of VCR and 10 mM of QC were dissolved into 1.5 ml of acetone–dichloromethane (0.8/1, v/v) mixture, which formed organic phase. The organic phase was emulsified with 3 ml of PVA205 solution (2%, w/v) by probe sonication at 50 W for 30 s in ice bath. The organic solvent was then rapidly evaporated under reduced pressure at 37 °C.

3.3. Characterization of the optimal nanoparticle formulation

3.3.1. Entrapment efficiencies and drug loading

The optimized VQ-PLGA-NPs improved significantly the drug incorporation, with an entrapment efficiency of $92.84 \pm 3.37\%$ for VCR and $32.66 \pm 2.92\%$ for QC ($n = 3$). The drug loadings were $0.0037 \pm 0.0001\%$ for VCR and $1.36 \pm 0.12\%$ for QC ($n = 3$). The molar ratio of VCR-to-QC entrapped into nanoparticles was approximately 1/1000, which might achieve a desirable efficacy in reversing resistance.

The optimized formulation parameters in this study were similar to those in the preparation of VV-PLGA-NPs, however, the entrapment efficiency of VCR in this VCR–QC–PLGA system was almost one time higher than that in the VCR–VRP–PLGA system ($55.35 \pm 4.22\%$, $n = 3$) [20]. This phenomenon was probably attributed to the different interaction between VCR–QC–PLGA–solvent and VCR–VRP–PLGA–solvent as discussed above. The entrapment efficiency of QC was less than 50% in various conditions of preparation variables. According to our previous study, one strategy was considered to increase QC encapsulation: the aqueous phase was saturated with NaCl (150 mM). However, the free drug QC would precipitate readily when the organic and aqueous phase mixtured and the QC entrapment was not modified, which was in accordance with dexamethasone encapsulation into PLGA nanoparticles [26]. It may be concluded that not all the hydrophobic drugs were easy to be entrapped into PLGA nanoparticles despite the hydrophobic nature of PLGA molecule.

3.3.2. Particle morphology and zeta potential

VQ-PLGA-NPs were characterized by PCS and exhibited a diameter of 139.5 ± 4.3 nm ($n = 3$). The polydispersity index of 0.095 ± 0.031 ($n = 3$) indicated a narrow size distribution. The PCS results of three batches of nanoparticles had no substantial difference, which demonstrated that the preparation process was reproducible and stable. TEM shows nanoparticles with mean diameter of 87 nm, spherical shape and smooth surface (Fig. 3). The size of the VQ-PLGA-NPs determined by PCS was not consistent with that determined by TEM, which was probably caused by the different mechanisms of the two methods. PCS and TEM were based on scattering (hydrodynamic radius) and diffraction technique in particle size measurement, respectively. The size detection of VQ-PLGA-NPs by PCS was carried out in aqueous state and in this case, nanoparticles were highly hydrated and the diameters detected by PCS were 'hydrated diameters', which are usually larger than their genuine diameters. In the case of TEM sample preparation, VQ-PLGA-NPs were stained with 2% (w/v) phosphotungstic acid and all the free water and even some of hydrated water were stained. This implied that the sizes of VQ-PLGA-NPs derived from TEM might be considerably smaller than their real diameters. The zeta potential of VQ-PLGA-NPs was slightly negative, with the value of -0.51 ± 0.08 mV ($n = 3$).

3.3.3. DSC

In order to describe the existing state of VCR and QC formulated in VQ-PLGA-NPs and elucidate the

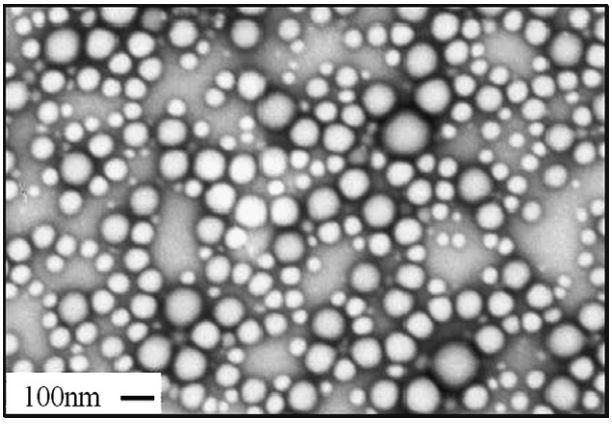

Fig. 3. Transmission electron micrograph of VQ-PLGA-NPs, scale bar: 100 nm.

mechanism of entrapment of VCR and QC into PLGA nanoparticles, DSC analysis was performed on blank nanoparticles, VCR, QC, VQ-PLGA-NPs and the physical mixture of three substances (VCR, QC and blank nanoparticles). From Fig. 4, we can see that two endothermic peaks were exhibited at 80.6 °C and 218.5 °C for VCR in Fig. 4B, while there were also two endothermic peaks at 84.4 °C and 218.7 °C for blank nanoparticles in Fig. 4A. Comparing the four curves of blank nanoparticles, VCR, VQ-PLGA-NPs and the physical mixture of three substances, no significant difference could be observed proving that VCR does not disperse within the PLGA nanoparticles. However, VQ-PLGA-NPs (C) had no endothermic peak of QC (D) at 122.8 °C, indicating that QC formulated in the nanoparticles existed as an amorphous state or a solid solution in the polymeric matrix.

3.3.4. In vitro release

Fig. 5 represented the release profiles of VCR and QC from VQ-PLGA-NPs. In contrast with the non-encapsulated drugs, there was a pronounced time prolongation of drugs release from nanoparticles. While about 100% of non-encapsulated drug was found in release medium after approximately 3 h, only 70% of drugs released from nanoparticles after 24 h. Moreover, these profiles showed a burst-release of drugs during the first 2 h of incubation,

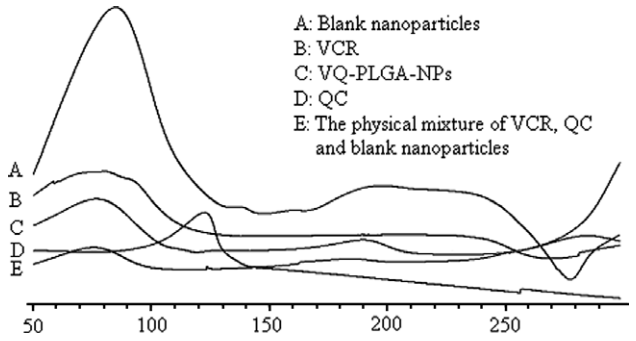

Fig. 4. DSC curves of blank nanoparticles, VCR, QC, VQ-PLGA-NPs and the physical mixture of three substances (VCR, QC and blank nanoparticles).

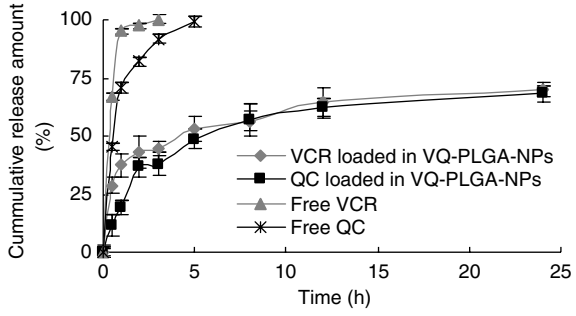

Fig. 5. In vitro release profile of VCR and QC in pH 7.4 phosphate buffer (mean ± SD, $n = 3$) from VQ-PLGA-NPs and the physical mixture of VCR and QC.

which have been reported by several authors for PLGA nanoparticles [32,33,35]. The fast release of VCR and QC was probably due to diffusion of drugs close to the surface of VQ-PLGA-NPs. According to the four release curves, it may be concluded that QC released slower than VCR in both the physical mixture of free drugs and VQ-PLGA-NPs. This may be caused by the poor water solubility of QC. The cumulative release percentage of QC loaded in VQ-PLGA-NPs was slightly lower than that of VCR at any time. However, the molar ratio of the two drugs releasing from VQ-PLGA-NPs was still around 1/1000 (VCR/QC), which could not affect the reversing efficacy.

4. Conclusions

In this paper, the influences of various processing variables on particle size and drug entrapment efficiencies were systematically assessed. It was concluded that formulation variables could be exploited in order to enhance the incorporation of dual agents into PLGA nanoparticles by O/W single emulsification method. Based on the optimal parameters, it was found that VQ-PLGA-NPs with expectable properties could be obtained. We point out for the first time that two drugs with different properties (VCR and QC, hydrophilic and hydrophobic molecule, respectively), could be simultaneously entrapped into PLGA nanoparticles, with a relatively high-entrapment efficiency and small size.

Optimization of formulation variables to control the size and drug entrapment efficiency of dual agent-loaded nanoparticles seems to be based on the same scientific principles as single agent-loaded nanoparticles prepared by O/W emulsion solvent evaporation method [21]. Both the emulsification process and the stability of emulsion globules were the most important factors to control the particle size, while both the drug–polymer interaction and the partition of drug in organic phase were the crucial factors to govern the drug entrapment efficiency. According to this study, to optimize MW of PLGA, PLGA concentration, W/O volume ratio, PVA concentration and A/D volume ratio can achieve smaller particle size. Additionally, to optimize L:G ratio of PLGA, initial drug content, A/D volume ratio, volume of organic solvent and pH of aqueous phase can enhance the drug entrapment efficiency. This systematic investigation reported here might promote the development of PLGA nanoparticles loaded with dual agents.

Acknowledgments

This research has received financial support from the National Natural Science Foundation of China (No. 30772668).

References

[1] A.H. Emmanuel, L.S. Patrick, A. Christine, P.M. Micheline, Impact of intraperitoneal, sustained delivery of paclitaxel on the expression of

P-glycoprotein in ovarian tumors, J. Control. Release 117 (2007) 20–27.
[2] E. Rowinsky, R.C. Donhower, Antimicrotubule agents, in: B.A. Chabner, D.L. Longo (Eds.), Cancer Chemotherapy and Biotherapy, Lippincot-Raven Publishers, Philadelphia, 1996, pp. 263–275.
[3] S.V. Ambudkar, C. Kimchi–Sarfaty, Z.E. Sauna, M.M. Gottesman, P-glycoprotein from genomics to mechanism, Oncogene 22 (2003) 7468–7485.
[4] P. Borst, N. Zelcer, K. van de Wetering, B. Poolman, On the putative co-transport of drugs by multidrug resistance proteins, FEBS Lett. 580 (2006) 1085–1093.
[5] P. Limtrakul, O. Khantamat, K. Pintha, Inhibition of P-glycoprotein function and expression by kaempferol and quercetin, J. Chemother. 17 (2005) 86–95.
[6] E.M. Leslie, Q. Mao, C.J. Oleschuk, R.G. Deeley, S.P. Cole, Modulation of multidrug resistance protein 1 (MRP1/ABCC1) transport and ATpase activities by interaction with dietary flavonoids, Mol. Pharmacol. 59 (2001) 1171–1180.
[7] J.J. van Zanden, H.M. Wortelboer, S. Bijlsma, A. Punt, M. Usta, P.J. Bladeren, I.M.C.M. Rietjens, N.H.P. Cnubben, Quantitative structure activity relationship studies on the flavonoid mediated inhibition of multidrug resistance proteins 1 and 2, Biochem. Pharmacol. 69 (2005) 699–708.
[8] M. Yoshikawa, Y. Ikegami, K. Sano, H. Yoshida, H. Mitomo, S. Sawada, T. Ishikawa, Transport of SN-38 by the wild type of human ABC transporter ABCG2 and its inhibition by quercetin, a natural flavonoid, J. Exp. Ther. Oncol. 4 (2004) 25–35.
[9] M. Ju-Ichi, Chemical study of citrus plants in the search for cancer chemopreventive agents, Yakugaku Zasshi 125 (2005) 231–254.
[10] R.L. Prior, Fruits and vegetables in the prevention of cellular oxidative damage, Am. J. Clin. Nutr. 78 (2003) 570–578.
[11] J. Marinina, A. Shenderova, S.R. Mallery, S.P. Schwendeman, Stabilization of vinca alkaloids encapsulated in poly(lactide-co-glycolide) microspheres, Pharm. Res. 17 (2000) 677–683.
[12] A.M. Julia, H. Roche, M. Berlion, Multidrug resistance circumvention by a new triazi-noaminopiperidine derivative S9788 in vitro, definition of the optimal schedule and comparison with verapamil, Br. J. Cancer 69 (1994) 868–875.
[13] S.K. Sahoo, V. Labhasetwar, Enhanced antiproliferative activity of transferrin-conjugated paclitaxel-loaded nanoparticles is mediated via sustained intracellular drug retention, Mol. Pharm. 2 (2005) 373–383.
[14] R.A. Jain, The manufacturing techniques of various drug loaded biodegradable poly(lactide–co–glycolide) (PLGA) devices, Biomaterials 21 (2000) 2475–2490.
[15] M. Vert, The complexity of PLAGA-based drug delivery systems, in: Proceedings of the International Conference on Advances in Controlled Delivery, Baltimore, MD, 1996, pp. 32–36.
[16] A. Budhian, S.J. Siegel, K.I. Winey, Production of haloperidol-loaded PLGA nanoparticles for extended controlled drug release of haloperidol, J. Microencapsul. 22 (2005) 773–785.
[17] U. Bilati, E. Allémann, Doelker, Eric., Development of a nanoprecipitation method intended for the entrapment of hydrophilic drugs into nanoparticles, Eur. J. Pharm. Sci. 24 (2005) 67–75.
[18] S.H. Choi, T.G. Park, G-CSF loaded biodegradable PLGA nanoparticles prepared by a single oil-in-water emulsion method, Int. J. Pharm. 311 (2006) 223–228.
[19] F. Tewes, E. Munnier, B. Antoon, L.N. Okassa, S. Cohen-Jonathan, H. Marchais, L. Douziech-Eyrolles, M. Soucé, P. Dubois, I. Chourpa, Comparative study of doxorubicin-loaded poly(lactide-co-glycolide) nanoparticles prepared by single and double emulsion methods, Eur. J. Pharm. Biopharm. 66 (2007) 488–492.
[20] X. Song, Yu Zhao, W. Wu, Y. Bi, Z. Cai, Q. Chen, Y. Li, S. Hou, PLGA nanoparticles simultaneously loaded with vincristine sulfate and verapamil hydrochloride: systematic study of particle size and drug entrapment efficiency, Int. J. Pharm. (2007), doi:10.1016/j.ijpharm.2007.08.034.
[21] A. Budhian, S.J. Siegel, K.I. Winey, Haloperidol-loaded PLGA nanoparticles: systematic study of particle size and drug content, Int. J. Pharm. 336 (2007) 367–375.
[22] T. Maribel, J.A. Maria, M.M.P. Madalena, M.B. Carlos, Development and characterization of PLGA nanospheres and nanocapsules containing xanthone and 3-methoxyxanthone, Eur. J. Pharm. Biopharm. 59 (2005) 491–500.
[23] P. Perugini, S. Simeoni, S. Scalia, I. Genta, T. Modena, B. Conti, F. Pavanetto, Effect of nanoparticle encapsulation on the photostability of the sunscreen agent, 2-ethylhexyl-*p*-methoxycinnamate, Int. J. Pharm. 246 (2002) 37–45.
[24] S. Stolnik, L. Illum, S.S. Davis, Long circulating microparticulate drug carriers, Adv. Drug Deliv. Rev. 16 (1995) 195–214.
[25] Y. Tabata, Y. Ikada, Phagocytosis of polymer microspheres by macrophages, Adv. Polym. Sci. 94 (1990) 107–141.
[26] T. Niwa, H. Takeuchi, T. Hino, N. Kunou, Y. Kawashima, Preparations of biodegradable nanospheres of water-soluble and insoluble drugs with D,L-lactide/glycolide copolymer by a novel spontaneous emulsification solvent diffusion method, and the drug release behavior, J. Control. Release 25 (1993) 89–98.
[27] S.A. Seo, G. Khang, J.M. Rhee, J. Kim, H.B. Lee, Study on in vitro release patterns of fentanyl-loaded PLGA microspheres, J. Microencapsul. 20 (2003) 569–579.
[28] S. Galindo-Rodriguez, E. Allemann, H. Fessi, E. Doelker, Physicochemical parameters associated with nanoparticle formation in the salting-out, emulsification-diffusion and nanoprecipitation methods, Pharm. Res. 21 (2004) 1428–1439.
[29] A. Nandi, D.V. Khakhar, A. Mehra, Coalescence in surfactant-stabilized emulsions subjected to shear flow, Langmuir 17 (2001) 2647–2655.
[30] S. Tesch, H. Schubert, Influence of increasing viscosity of the aqueous phase on the short-term stability of protein stabilized emulsions, J. Food Eng. 52 (2002) 305–312.
[31] F. Boury, T. Ivanova, I. Panaiotov, J.E. Proust, A. Bois, J. Richou, Dynamic properties of poly(DL-lactide) and polyvinyl alcohol monolayers at the air/water and dichloromethane/water interfaces, J. Colloid Interf. Sci. 169 (1995) 380–392.
[32] C. Gómez-Gaete, N. Tsapis, M. Besnard, A. Bochot, E. Fattal, Encapsulation of dexamethasone into biodegradable polymeric nanoparticles, Int. J. Pharm. 331 (2007) 153–159.
[33] T. Govender, S. Stolnik, M.C. Garnett, L. Illum, S.S. Davis, PLGA nanoparticles prepared by nanoprecipitation, drug loading and release studies of a water soluble drug, J. Control. Release 57 (1999) 171–185.
[34] M.R. Webb, S.E. Ebeler, Comparative analysis of topoisomerase IB inhibition and DNA intercalation by flavonoids and similar compounds: structural determinates of activity, Biochem. J. 384 (2004) 527–541.
[35] R.M. Mainardes, R.C. Evangelista, PLGA nanoparticles containing praziquantel: effect of formulation variables on size distribution, Int. J. Pharm. 290 (2005) 137–144.